Mechanics of Advanced Composite Structures 8 (2021) 77-86

Mechanics of Advanced Composite Structures

Semnan University

journal homepage: http://MACS.journals.semnan.ac.ir

Assessment of Hydrostatic Stress and Thermo Piezoelectricity in a Laminated Multilayered Rotating Hollow Cylinder

S. Mahesh [a], R. Selvamani [b*], F. Ebrahami [c]

[a] *Department of Mathematics, Kathir College of Engineering, Coimbatore, 641062, India.*
[b] *Department of Mathematics, Karunya Institute of Technology and Sciences, Coimbatore, 641114, India.*
[c] *Department of Mechanical Engineering, Imam Khomeini International University Qazvin, Iran.*

KEYWORDS

Initial hydrostatic stress
Thermoelasticity
Longitudinal waves
Bessel function

ABSTRACT

In this paper, we built a mathematical model to study the influence of the initial stress on the propagation of waves in a hollow infinite multilayered composite cylinder. The elastic cylinder assumed to be made of inner and outer thermo piezoelectric layer bonded together with Linear Elastic Material with Voids (LEMV) layer. The model described by the equations of elasticity, the effect of the initial stress and the framework of linearized, three-dimensional theory of thermo elasticity. The displacement components obtained by founding the analytical solutions of the motion's equations. The frequency equations that include the interaction between the composite hollow cylinders are obtained by the perfect-slip boundary conditions using the Bessel function solutions. The numerical calculations carried out for the material PZT-5A and the computed non-dimensional frequency against various parameters are plotted as the dispersion curve by comparing LEMV with Carbon Fiber Reinforced Polymer (CFRP). From the graph, it is clear that those are analyzed in the presence of hydrostatic stress is compression and tension.

1. Introduction

Composite materials are generally utilized in en-gineering structures because of their predominance over the basic materials in applications requiring high quality and solidness in lightweight parts. Thusly, the portrayal of their mechanical conduct is taking imperative part in basic plan. Procedures that incite transversely isotropic flexible properties in them make most cylindrical parts, for example, poles, wires, cylinders, funnels and strands. Displaying the proliferation of waves in these parts is significant in different applications, including ultrasonic nondestructive assessment systems, progression of room explore and numerous others. Smart materials are normally prestressed during the assembling procedure. As initial stresses are indivisible in surface acoustic wave gadgets and resonators, investigation of such impacts has been finished with various methodologies. A few creators have considered wave engendering in prestressed piezoelectric structure.

Soniya Chaudhary et al. [1] derived secular equation of SH waves propagating in prestressed and rotating piezo-composite structure with imperfect interface. Abhinav Singhal et al. [2] analyticaly analysed interfacial imperfection study in pres-stressed rotating multiferroic cylindrical tube with wave vibration. Lotfy and El-Bary [3] discussed photothermal excitation for a semiconductor medium due to pulse heat flux and volumetric source of heat with thermal memory. Lotfy [4] discovered a novel model for photothermal excitation of variable thermal conductivity semiconductor elastic medium subjected to mechanical ramp type with two-temperature theory and magnetic feld. Soniya Chaudhary et al. [5] studied anatomy of flexoelectricity in micro plates with dielectrically highly/weakly and mechanically complaint interface. Ebrahimi et al. [6] discussed Magneto-electro-elastic analysis of piezoelectric–flexoelectric nanobeams rested on silica aerogel foundation. Abhinav Singhal et al. [7] investigate mechanics of 2D Elastic Stress Waves Propaga-

*Corresponding author. Tel.: +91-9842647487
E-mail address: selvam1729@gmail.com

DOI: 10.22075/MACS.2020.19273.1230
Received 2019-12-09; Received in revised form 2020-05-27; Accepted 2020-06-19

tion Impacted by Concentrated Point Source Disturbance in Composite Material Bars. Lotfy [8] discover a novel model of photothermal diffusion (PTD) for polymer nano-composite semiconducting of thin circular plate. Placidi and Hutter [9] studied thermodynamics of Polycrystalline materials treated by the theory of mixtures with continuous diversity. Altenbach and Eremeyev [10] discussed vibrtion analysis of non-linear 6-parameter prestressed shells. Sonal Nirwal et al. [11] analysised of different boundary types on wave velocity in bedded piezostructure with flexoelectric effect. Lotfy and Wafaa Hassan [12] discovered the effect of rotation for two-temperature generalized thermoelasticity of two-dimensional under thermal shock problem.Abhinav Singhal et al. [13] studied Liouville-Green approximation: an analytical approach to study the elastic wave's vibrations in composite structure of piezo material.Soniya Chaudhary and Abhinav Singhal [14], [15] discussed analytic model for Rayleigh wave propagation in piezoelectric layer overlaid orthotropic substratum and surface wave propagation in functionally graded piezoelectric material. Abbas and Othman [16] generalized thermoelastic interacon in a fiber-reinforced anisotropic half-space under hydrostatic initial stress. Othman and Lotfy [17] discussed the influence of gravity on 2-D problem of two temperatures generalized thermoelastic medium with thermal relaxation. Abo-Dahab et al. [18] discovered rotation and magnetic field effect on surface waves propagation in an elastic layer lying overa generalized thermoelastic diffusive half-space with imperfect boundary. Hobinyand and Abbas [19] studied analytical solution of magneto-thermoelastic interaction in a fiber-reinforced anisotropic material. Manoj Kumar Singh et al. [20] discussing approximation of surface wave velocity in smart composite structure using Wentzel–Kramers–Brillouin method. Othman, Abo-Dahab, and Lotfy [21] investigate gravitational effect and initial stress on generalized magneto-thermomicrostretch elastic solid for different theories. Abo-Dahab and Lotfy [22] designed two-temperature plane strain problem in a semiconducting medium under photo thermal theory. Abo-Dahab [23] discussed reflection of P and SV waves from stress-free surface elastic half-space under influence of magnetic field and hydrostatic initial stress without energy dissipation. Abhinav Singhal et al. [24], [25] studied Stresses produced due to moving load in a prestressed piezoelectric substrate and approximation of surface wave frequency in piezo-composite structure. Alireza Mohammadi et.al [26] discover the results of influence of viscoelastic foundation on dynamic behaviour of the double walled cylindrical inhomogeneous micro shell using MCST and with the aid of GDQM. Ebrahimi et.al [27] studied the impacts of thermal buckling and forced vibration characteristics of a porous GNP reinforced nanocomposite cylindrical shell. Habibi, Hashemabadi and Safarpour [28] discussed the vibration analysis of a high-speed rotating GPLRC nanostructure coupled with a piezoelectric actuator. MostafaHabibi et.al [29] studied stability analysis of an electrically cylindrical nanoshell reinforced with graphene nanoplatelets.MehranSafarpoura et.al [30] analysics frequency characteristics of FG-GPLRC viscoelastic thick annular plate with the aid of GDQM.

In this paper, we have built a mathematical model to study the effect of imposing thermal field on longitudinal wave propagation in a hollow multilayered composite cylinder under the influence of initial hydrostatic stress. The cylinder is made of tetragonal system material, such as PZT-5A. The displacement components are obtained by founding the analytical solutions of the motion's equations. After applying suitable boundary conditions, the frequency equation is presented as a determinant with elements containing Bessel functions. The numerical computations obtained the roots of frequency equations. The dispersion curve carried for various parameters.

2. Formulation of the problem and basic equations

Longitudinal wave propagation in a homogeneous, transversely isotropic cylinder of tetragonal elastic material of inner and outer radius x and a subjected to an axial thermal and electric field is considered. The cylinder is treated as a perfect conductor and the regions inside and outside the elastic material is assumed to be vacuumed. The medium is assumed to be rotating with uniform angular velocity $\overline{\Omega}$. The displacement field, in cylindrical coordinates (r, θ, z) is given by

$$\sigma^{l}{}_{rr,r} + \sigma^{l}{}_{rz,z} + r^{-1}(\sigma^{l}{}_{rr}) + \rho(\overline{\Omega} \times (\overline{\Omega} \times \overline{u}) + 2(\overline{\Omega} \times \overline{u}_{,t})) = \rho u_{,tt} \quad (1a)$$

$$\sigma^{l}{}_{rz,r} + \sigma^{l}{}_{zz,z} + r^{-1}\sigma^{l}{}_{rz} + \rho(\overline{\Omega} \times (\overline{\Omega} \times \overline{u}) + 2(\overline{\Omega} \times \overline{u}_{,t})) = \rho w_{,tt} \quad (1b)$$

The electric displacement equation

$$\frac{1}{r}\frac{\partial}{\partial r}(rD^{l}{}_{r}) + \frac{\partial D^{l}{}_{z}}{\partial z} = 0 \quad (1c)$$

The heat conduction equation

$$K_1\left(T^l{}_{,rr}+r^{-1}T^l{}_{,r}+r^{-2}T^l{}_{,\theta\theta}\right)+K_3T^l{}_{,zz}-\rho c_vT^l{}_{,t}=T_0\frac{\partial}{\partial t}\left[\beta_1(e^l{}_{rr}+e^l{}_{\theta\theta})+\beta_3e^l{}_{,zz}-p_3\,\phi_{,z}\right] \quad (1d)$$

The stress strain relations are given as follows

$$\sigma^l{}_{rr}=c_{11}e^l{}_{rr}+c_{12}e^l{}_{\theta\theta}+c_{13}e^l{}_{zz}-\beta_1T^l-e_{31}\varphi_z^l$$

$$\sigma^l{}_{zz}=c_{13}e^l{}_{rr}+c_{13}e^l{}_{\theta\theta}+c_{33}e^l{}_{zz}-\beta_3T^l-e_{33}\varphi_z^l$$

$$\sigma^l{}_{rz}=c_{44}e^l{}_{rz} \quad (2)$$

$$D_r=e_{15}e^l{}_{rz}+\varepsilon_{11}\varphi^l{}_r$$

$$D_z=e_{31}(e^l{}_{rr}+e^l{}_{\theta\theta})+e_{33}e^l{}_{zz}+\varepsilon_{33}\varphi^l{}_z+p_3T$$

Where $\sigma^l{}_{rr},\sigma^l{}_{r\theta},\sigma^l{}_{rz},\sigma^l{}_{\theta\theta},\sigma^l{}_{zz},\sigma^l{}_{\theta z}$ are the stress and $e^l{}_{rr},e^l{}_{zz},e^l{}_{\theta\theta},e^l{}_{r\theta},e^l{}_{z\theta},e^l{}_{rz}$ are the strain components, T is the temperature change about the equilibrium temperature $c_{11},c_{12},c_{13},c_{33},c_{44},c_{66}$ are the five elastic constants,β_1,β_3 and K_1,K_3 respectively thermal expansion coefficients and thermal conductivities along and perpendicular to the symmetry, ρ is the mass density, c_v is the specific heat capacity ,p_3 is the pyroelectric effect.

The strains $e^l{}_{ij}$ related to the displacements given by [32]

$$e^l{}_{rr}=u^l{}_{,r}\qquad e^l{}_{\theta\theta}=r^{-1}\left(u^l+v^l{}_{,\theta}\right),\quad e^l{}_{zz}=w^l{}_{,z}$$

$$e^l{}_{r\theta}=v^l{}_r-r^{-1}\left(v^l-u^l{}_{,\theta}\right),\quad e^l{}_{z\theta}=v^l{}_{,z}+r^{-1}w^l{}_{,\theta},\qquad e^l{}_{rz}=w^l{}_{,r}+u^l{}_{,z} \quad (3)$$

Substitution of the Eqs. (3) and (2) into Eqs. (1) results in the following three-dimensional equation of motion, heat and electric conduction. We note that the first two equations under the influence hydrostatical stress become [31]:

$$c_{11}\left(u^l{}_{,rr}+r^{-1}u^l{}_{,r}+r^{-2}u^l\right)+c_{13}w^l{}_{,rz}+c_{44}\left(u^l{}_{,zz}+w^l{}_{,rz}\right)+(e_{15}+e_{31})\varphi^l_{,rz}-p_0\left(u^l{}_{,rr}+r^{-1}u^l{}_{,r}+r^{-2}u^l+u^l{}_{,zz}\right)-\beta_1T^l{}_{,r}+\rho(\Omega^2u+2\Omega w_{,t})=\rho u_{,tt} \quad (4a)$$

$$(c_{44}+c_{13})\left(u^l{}_{,rz}+r^{-1}u^l{}_{,z}\right)+c_{33}\left(w^l{}_{,zz}\right)+c_{44}\left(w^l{}_{,rr}+r^{-1}w^l{}_{,r}\right)+e_{15}\left(\varphi^l_{,rr}+r^{-1}\varphi_{,r}\right)-p_0\left(w^l{}_{,rr}+r^{-1}w^l{}_{,r}+w^l{}_{,zz}\right)-\beta_3T^l{}_{,r}+\rho(\Omega^2w+2\Omega u_{,t})=\rho w_{,tt} \quad (4b)$$

$$r^{-1}e_{15}\left(w^l_{,rr}+u^l_{,rz}\right)+\varepsilon_{11}\varphi^l_{,r}+e_{13}u^l_{,rz}+r^{-1}u^l_r+e_{33}w^l_{,zz}+\varepsilon_{33}\varphi^l_{,z}+p_3T=0 \quad (4c)$$

$$k_{11}\left(T^l{}_{,rr}+r^{-1}T^l{}_{,r}\right)+k_{33}T^l{}_{,zz}-T_0dT^l{}_{,t}=T_0[\beta_1\left(u^l{}_{,rt}+r^{-1}u^l{}_{,t}\right)+\beta_3w^l{}_{,z}] \quad (4d)$$

Where k_{ij} is heat conduction coefficient, $d=\frac{\rho C_v}{T_0}$, u and w are the displacements along r, z direction, ρ is the mass density and t is the time.

The solutions of Eq. (4) is considered in the form

$$u^l=U^l{}_{,r}\exp\{i(kz+pt)\}$$

$$w^l=\left(\frac{i}{h}\right)W^l\exp\{i(kz+pt)$$

$$\varphi^l=\left(\frac{ic_{44}}{ae_{33}}\right)E^l\exp\{\,i(kz+pt)\}$$

$$T^l=\left(\frac{c_{44}}{\beta_3}\right)\left(\frac{T^l}{h^2}\right)\exp\{i(kz+pt)\} \quad (5)$$

Where, u^l,w^l,φ^l,T^l are displacement potentials, k is the wave number, p is the angular frequency and $i=\sqrt{-1}$. We introduce the non-dimensional quantities $x=\frac{r}{a},\varepsilon=ka,c=\rho p$ 'a' is the geometrical parameter of the composite hollow cylinder. $\bar{c}_{11}={}^{c_{11}}/_{c_{44}},\bar{c}_{13}={}^{c_{13}}/_{c_{44}},\bar{c}_{33}={}^{c_{33}}/_{c_{44}},\bar{c}_{66}={}^{c_{66}}/_{c_{44}},\bar{\beta}={}^{\beta_1}/_{\beta_3},\bar{k}_i=\frac{(\rho c_{44})^{\frac{1}{2}}}{\beta_3^2T_0a\Omega}$,

Substituting Eqs. (5) in Eqs. (4), we obtain:

$$[(\bar{c}_{11}-p_0)\nabla^2-(1-p_0)\varepsilon^2+\zeta^2+\chi^2+\beth]U^l-[\varepsilon(1+\bar{c}_{13})]W^l-\varepsilon(\bar{e}_{31}+\bar{e}_{15})E^l-\bar{\beta}T^l=0 \quad (6a)$$

$$[\varepsilon(1+\bar{c}_{13})\nabla^2]U^l+[(1-p_0)\nabla^2-(\bar{c}_{33}-p_0)\varepsilon^2+\zeta^2+\chi^2+\beth]W^l+(\bar{e}_{15}\nabla^2-\varepsilon^2)E^l-\varepsilon T^l=0 \quad (6b)$$

$$\varepsilon((\bar{e}_{31}+\bar{e}_{15})\nabla^2U^l+(\bar{e}_{15}\nabla^2+\varepsilon^2)W^l-(K_{11}^2\nabla^2+K_{33}\varepsilon^2)E^l-p\varepsilon T^l=0 \quad (6c)$$

$$\bar{\beta}\nabla^2U^l+\varepsilon W^l-p\varepsilon E^l+\left(i\bar{K}_1\nabla^2+i\bar{K}_3\varepsilon^2-\bar{d}\right)T^l=0 \quad (6d)$$

The above Eqs. [6] rearranged in the following form

$$\begin{vmatrix}(\bar{c}_{11}-p_0)\nabla^2-s_1+A_1 & -A_2 & A_3 & -A_4\\ A_2 & (1-p_0)\nabla^2-s_2+A_1 & e_{15}^2\nabla^2+A_5 & A_6\\ A_3\nabla^2 & e_{15}^2\nabla^2+A_5 & K_{11}^2\nabla^2+A_7 & -A_8\\ A_4\nabla^2 & A_6 & -A_8 & i\bar{K}_1\nabla^2+A_9\end{vmatrix}\times(U^l,W^l,E^l,T^l)=0 \quad (7)$$

Where

$A_1 = \zeta^2 + \chi^2 + ↄ, A_2 = \varepsilon(1 + \bar{c}_{13}), A_3 = \varepsilon(\bar{e}_{31} + \bar{e}_{15}),\ A_4 = -\beta, A_5 = \varepsilon^2, A_6 = \varepsilon,\ A_7 = K_{33}^2\varepsilon^2\quad A_8 = -p^l\varepsilon\ , A_9 = i\bar{k}_3\varepsilon^2 - \bar{d}, s_1 = (1 - p_0)\varepsilon^2\ ,\ s_2 = (\bar{c}_{33} - p_0)\varepsilon^2\ .$

Evaluating the determinant given in Eq. (7), we obtain a partial differential equation of the form:

$$(A\nabla^8 + B\nabla^6 + C\nabla^4 + D\nabla^2 + E)(U^l\ W^l\ E^l\ T^l)^T = 0 \quad (8)$$

Factorizing the relation given in Eq. (8) into biquadratic equation for$\left(\alpha^l{}_j a\right)^2$, i=1, 2, 3, 4 the solutions for the symmetric modes are obtained as

$$U^l = \sum_{j=1}^{4}\left[A_j J_n(\alpha_j x) + B_j y_n(\alpha_j x)\right],$$

$$W^l = \sum_{j=1}^{4} a^l{}_j\left[A_j J_n(\alpha_j x) + B_j y_n(\alpha_j x)\right],$$

$$E^l = \sum_{j=1}^{4} b^l{}_j\left[A_j J_n(\alpha_j x) + B_j y_n(\alpha_j x)\right],$$

$$T^l = \sum_{j=1}^{4} c^l{}_j\left[A_j J_n(\alpha_j x) + B_j y_n(\alpha_j x)\right],$$

Here $(\alpha_i^l ax) > 0$, for $(i = 1,2,3,4)$ are the roots of algebraic equation

$$\left(A\left(\alpha^l{}_j a\right)^8 + B\left(\alpha^l{}_j a\right)^6 + C\left(\alpha^l{}_j a\right)^4 + D\left(\alpha^l{}_j a\right)^2 + E\right)(U^l, W^l, E^l, T^l) = 0 \quad (10)$$

The solutions corresponding to the root $(\alpha_i a)^2 = 0$ not considered here, since $J_n(0)$ is zero, except $n = 0$. The Bessel function J_n is used when the roots$(\alpha_i a)^2$,$(i = 1,2,3,4)$ are real or complex and the modified Bessel function I_n is used when the roots $(\alpha_i a)^2, (i = 1,2,3,4)$ are imaginary.

The constants $a^l{}_j, b^l{}_j$ and $c^l{}_j$ defined in Equation (10) can be calculated from the following equations

$$[(\bar{c}_{11} - p_0)\nabla^2 - (1 - p_0)\varepsilon^2 + \zeta^2 + \chi^2 + ↄ] - \varepsilon(1 + \bar{c}_{13})a^l{}_j - \varepsilon(\bar{e}_{31} + \bar{e}_{15})b^l{}_j - \bar{\beta}c^l{}_j = 0$$

$$\varepsilon(1 + \bar{c}_{13})\nabla^2 + [(1 - p_0)\nabla^2 - (\bar{c}_{33} - p_0)\varepsilon^2 + \zeta^2 + \chi^2 + ↄ]a^l{}_j + (\bar{e}_{15}\nabla^2 - \varepsilon^2)b^l{}_j - \varepsilon c^l{}_j = 0$$

$$\varepsilon((\bar{e}_{31} + \bar{e}_{15})\nabla^2 + (\bar{e}_{15}\nabla^2 + \varepsilon^2)a^l{}_j - (K_{11}^2\nabla^2 + K_{33}\varepsilon^2)b^l{}_j - p\varepsilon c^l{}_j = 0$$

$$\bar{\beta}\nabla^2 + \varepsilon a^l{}_j - p\varepsilon b^l{}_j + \left(i\bar{K}_1\nabla^2 + i\bar{K}_3\varepsilon^2 - \bar{d}\right)c^l{}_j = 0$$

3. Equation of Motion for Linear Elastic Materials with Voids LEMV

The displacement equations of motion and equation of equilibrated inertia for an isotropic LEMV are

$$(\lambda + 2\mu)\left(u_{,rr} + r^{-1}u_{,r} - r^{-2}u\right) + \mu u_{,zz} + (\lambda + \mu)w_{,zz} + \beta E_{,r} = \rho u_{tt} \quad (11a)$$

$$(\lambda + \mu)\left(u_{,rz} + r^{-1}u_{,z}\right) + \mu\left(w_{,rr} + r^{-1}w_{,r}\right) + (\lambda + 2\mu)w_{,zz} + \beta E_{,z} = \rho w_{,tt} \quad (11b)$$

$$-\beta\left(u_{,r} + r^{-1}u\right) - \beta w_{,z} + \alpha\left(E_{,rr} + r^{-1}E_{,r} + \phi_{,zz}\right) - \delta k E_{,tt} - \omega E_{,t} - \xi E = 0 \quad (11c)$$

The stress in the LEMV core materials are

$$\sigma_{,rr} = (\lambda + 2\mu)u_{,r} + \lambda r^{-1}u + \lambda w_{,z} + \beta\phi$$

$$\sigma_{rz} = \mu\left(u_{,t} + w_{,r}\right)$$

The solution for Eq. (11) is taken as

$$u = U_{,r}expi(kz + pt)$$

$$w = \left(\frac{i}{h}\right)Wexpi(kz + pt) \quad (12)$$

$$E = \left(\frac{1}{h^2}\right)E\ expi(kz + pt)$$

The above solution in (11) and dimensionless variables x and ε, equation can be simplified as

$$\begin{vmatrix}(\lambda + 2\mu)\nabla^2 + M_1 & -M_2 & M_3\\ M_2\nabla^2 & \bar{\mu}\nabla^2 + M_4 & M_5\\ -M_3\nabla^2 & M_5 & \alpha\nabla^2 + M_6\end{vmatrix} \times (u, w, E) = 0 \quad (13)$$

Where $\nabla^2 = \frac{\partial^2}{\partial x^2} + \frac{1}{x}\frac{\partial}{\partial x}$

$M_1 = \frac{\rho}{\rho^1}(ch)^2 - \bar{\mu}\varepsilon^2\ ,\quad M_2 = (\bar{\lambda} + \bar{\mu})\varepsilon\ ,M_3 = \bar{\beta},$
$M_4 = \frac{\rho}{\rho^1}(ch)^2 - (\bar{\lambda} + \bar{\mu})\varepsilon^2\ ,M_5 = \bar{\beta}\varepsilon$

$$M_6 = \frac{\rho}{\rho^1}(ch)^2\bar{k} - \bar{\alpha}\varepsilon^2 - i\bar{\omega}(ch) - \bar{\xi}$$

The Eq. (13) can specified as,

$$(\nabla^6 + P\nabla^4 + Q\nabla^2 + R)(U, W, E) = 0 \quad (14)$$

Thus, the solution of Eq. (14) is as follows,

$$U = \sum_{j=1}^{3}\left[A_j J_0(\alpha_j x) + B_j y_0(\alpha_j x)\right],$$

$$W = \sum_{j=1}^{3} a_j\left[A_j J_0(\alpha_j x) + B_j y_0(\alpha_j x)\right],$$

$$E = \sum_{j=1}^{3} b_j\left[A_j J_0(\alpha_j x) + B_j y_0(\alpha_j x)\right],$$

$(\alpha_j x)^2$ are the roots of the equation when replacing $\nabla^2 = -(\alpha_j x)^2$. The arbitrary constant a_j and b_j are obtained from

$$M_2\nabla^2 + (\bar{\mu}\,\nabla^2 + M_4)a_j + M_5 b_j = 0,$$

$$-M_3\nabla^2 + M_5 a_j + (\alpha\nabla^2 + M_6)b_j = 0$$

By taking the void volume fraction E=0, and the lame's constants as $\lambda = c_{12}, \mu = \frac{c_{11}-c_{12}}{2}$ in the Eq. (11) we got the governing equation for CFRP core material.

4. Boundary conditions and frequency equations

The frequency equations can obtain for the following boundary condition

- On the traction free inner and outer surface $\sigma^l{}_{rr} = \sigma^l_{rz} = E^l = T^l = 0$ with $l = 1,3$
- At the interface $\sigma^l_{rr} = \sigma_{rr}; \sigma^l_{rz} = \sigma_{rz}; E^l = 0; T^l = 0; D^l = 0.$

Substituting the above boundary condition, we obtained as a 22×22 determinant equation

$$\left|(Y_{ij})\right| = 0\ , (i, j = 1,2,3, \ldots .22) \qquad (15)$$

At $x = x_0$ Where $j = 1,2,3,4$

$$Y_{1j} = 2\bar{c}_{66}\left(\frac{\alpha_j^1}{x_0}\right)J_1(\alpha^1{}_j x_0) - \left[(\alpha^1{}_j a)^2\bar{c}_{11} + \zeta\bar{c}_{13}a^l{}_j + \bar{e}_{31}\zeta b^l{}_j + \bar{\beta}c^l{}_j\right]J_0(\alpha^1{}_j a x_0)$$

$$Y_{2j} = \left(\zeta + a_j^1 + \bar{e}_{15}b_j^1\right)(\alpha_j^1)\,J_1(\alpha^1{}_j x_0)$$

$$Y_{3j} = b_j^1 J_0(\alpha^1{}_j x_0)$$

$$Y_{4j} = \frac{h_j^1}{x_0}J_0(\alpha^1{}_j x_0) - (\alpha_j^1)\,J_1(\alpha^1{}_j x_0)$$

In addition, the other nonzero elements $Y_{1,j+4}, Y_{2,j+4}, Y_{3,j+4}$ and $Y_{4,j+4}$are obtained by replacing J_0 by $J_1$and Y_0 byY_1.

At $x = x_1$

$$Y_{5j} = 2\bar{c}_{66}\left(\frac{\alpha_j^1}{x_1}\right)J_1(\alpha^1{}_j x_1) - \left[(\alpha^1{}_j a)^2\bar{c}_{11} + \zeta\bar{c}_{13}a^l{}_j + \bar{e}_{31}\zeta b^l{}_j + \bar{\beta}c^l{}_j\right]J_0(\alpha^1{}_j a x_1)$$

$$Y_{5,j+8} = -[2\bar{\mu}\left(\frac{\alpha_j}{x_1}\right)J_1(\alpha x_1) + \left\{-\left(\bar{\lambda}+\bar{\mu}\right)(\alpha_j)^2 + \bar{\beta}b_j - \bar{\lambda}\zeta a_j\right\}J_0(\alpha_j x_1)$$

$$Y_{6j} = \left(\zeta + a_j^1 + \bar{e}_{15}b_j^1\right)(\alpha_j^1)\,J_1(\alpha^1{}_j a x_1)$$

$$Y_{6,j+8} = -\bar{\mu}(\zeta + a_j)(\alpha_j)J_1(\alpha_j x_1)$$

$$Y_{7j} = (\alpha_j^l)J_1(\alpha_j^l x_1)$$

$$Y_{7,j+8} = -(\alpha_j)J_1(\alpha^l{}_j x_1)$$

$$Y_{8j} = a_j^l J_0(\alpha_j^l x_1)$$

$$Y_{8,j+8} = -a_j^l J_0(\alpha_j^l x_1)$$

$$Y_{9j} = b_j^l J_0(\alpha_j^l x_0)$$

$$Y_{10j} = e_j(\alpha_j)J_1(\alpha_j^1 x_1)$$

$$Y_{11j} = \frac{c_j^l}{x_1}J_0(\alpha_j^l x_1) - (\alpha_j^l)J_1(\alpha_j^l x_1)$$

and the other nonzero element at the interfaces $x = x_1$ can be obtained on replacing J_0 by J_1 and Y_0 by Y_1 in the above elements. They are $Y_{i,j+4}, Y_{i,j+8}, Y_{i,j+11}, Y_{i,j+14,}$ $(i = 5,6,7,8)$ and $Y_{9,j+4}, Y_{10,j+4}, Y_{11,j+4,}$. At the interface $x = x_2$, nonzero elements along the following rows Y_{ij} , $(i = 12,13, \ldots ,18$ and $j = 8,9, \ldots ,20)$ are obtained on replacing x_1 by $x_2$and superscript 1 by 2 in order. Similarly, at the outer surface $x = x_3$, the nonzero elements Y_{ij} , $(i = 19,20,21,22$ and $j = 14,15,, \ldots ,22)$ can be had from the nonzero elements of first four rows by assigning x3 for x0 and superscript 2 for 1. In the case of without voids in the interface region, the frequency equation obtained by taking $E = 0$ in Eq. (11) which reduces to a 20 x 20 determinant equation. The frequency equations derived above are valid for different inner and outer materials of 6mm class and arbitrary thickness of layers.

5. Numerical results and discussion

The frequency equation given in Eq. (15) is transcendental in nature with unknown frequency and wave number. The solutions of the frequency equations obtained numerically by fixing the wave number. The material chosen for the numerical calculation is PZT-5A. The material properties of PZT-5A used for the numerical calculation given below:

$C_{11} = 13.9 \times 10^{10}\ \mathrm{Nm^{-2}};\ C_{12} = 7.78 \times 10^{10}\ \mathrm{Nm^{-2}};$
$C_{13} = 7.43 \times 10^{10}\ \mathrm{Nm^{-2}};\ C_{33} = 11.5 \times 10^{10}\ \mathrm{Nm^{-2}};$
$C_{44} = 2.56 \times 10^{10}\ \mathrm{Nm^{-2}};\ C_{66} = 3.06 \times 10^{10}\ \mathrm{Nm^{-2}};$
$\beta_1 = 1.52 \times 10^6\ \mathrm{NK^{-1}m^{-2}};\ T_0 = 298\mathrm{K};$
$\beta_3 = 1.53 \times 10^6\ NK^{-1}m^{-2},\ c_v = 420\mathrm{Jkg^{-1}K^{-1}}$
$p_3 = -452 \times 10^{-6}\ \mathrm{CK^{-1}m^{-2}}; e_{13} = -6.98\mathrm{Cm^{-2}}$
$K_1 = K_3 = 1.5\mathrm{Wm^{-1}K^{-1}};\ e_{33} = 13.8\mathrm{Cm^{-2}}$
$e_{15} = 13.4\mathrm{Cm^{-2}}\ ;\rho = 7750\mathrm{Kgm^{-2}};$
$\varepsilon_{11} = 60.0 \times 10^{-10}\mathrm{C^2N^{-1}m^{-2}};$
$\varepsilon_{33} = 5.47 \times 10^{-10}\mathrm{C^2N^{-1}m^{-2}}.$

The non-dimensional frequency versus the wave number and thickness h are plotted in Figs 2–5, which delineate the impacts of the underlying hydrostatic stress on the longitudinal vibrations of a hollow circular cylinder for the benefit of turning parameter Ω. From the Figs 2 and 3 there are a type of comparative changes gathered in non dimensional frequency against the wave number which differing in rotational speed Ω. whereas,the non dimensional frequency expanding at the same time for the higher estimations of wave number to arrive at as far as possible and again diminished in Fig: 1. From the Figs 4 and 5, there is a comparative change, which can be watched above all in non-dimensional frequency against the thickness which shifting in rotational speed Ω.The study represents the conduct of turning at first focused on hollow cylinder. Not withstanding the idea of non-dimensional frequency against hydrostatic pressure (p_0=-5, 0, 5×10^6) is watched.

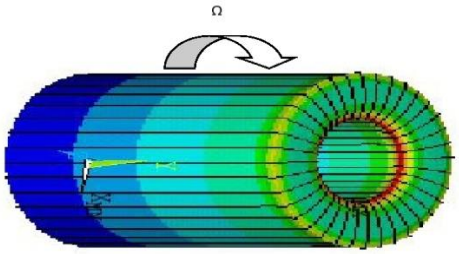

Fig .1. Geometry of the problem

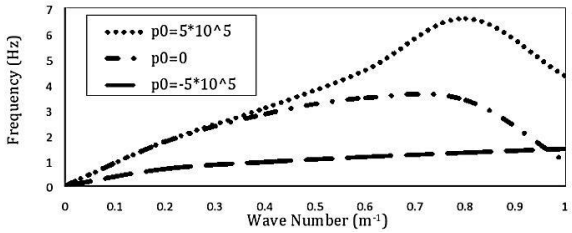

Fig. 2. Variation of frequency versus wave number against hydrostatic stress p0 with Ω=0.

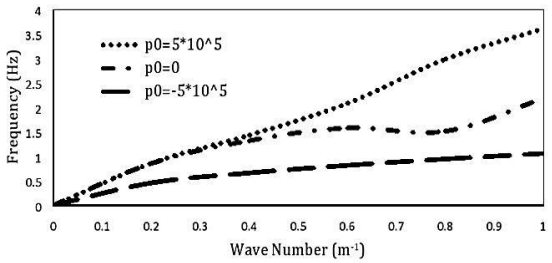

Fig. 3. Variation of frequency versus wave number against hydrostatic stress p0 with Ω=0.4.

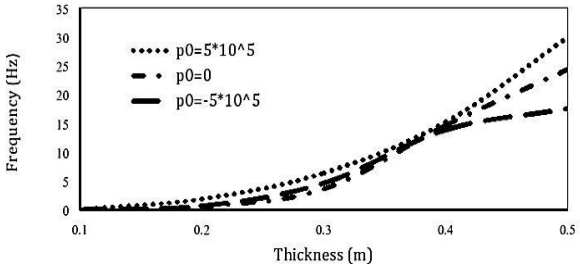

Fig. 4. Variation of frequency versus Thickness against hydrostatic stress p0 with Ω=0

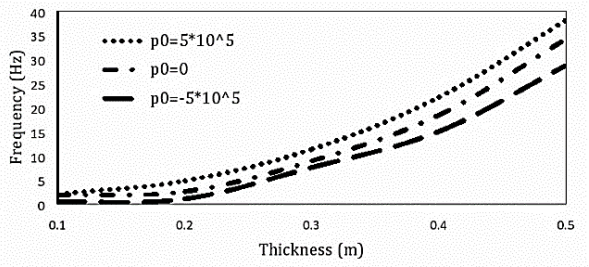

Fig. 5. Variation of frequency versus Thickness against hydrostatic stress p0 with Ω=0.4

The non-dimensional frequency versus the wave number and thickness h is plotted in Figs 6–9, which represent the impacts of the underlying hydrostatic stress on the longitudinal vibrations of a hollow circular cylinder for the estimation of Electric parameter E. From the Figs 6 and 7 there is a slight change happened in non-dimensional frequency against the wave number which shifting in Electric parameter E and the equivalent, which shows in hydrostatic pressure. Despite the fact that, the non dimensional frequency which stays consistent by expanding in wave number. From the Figs 8 and 9 it is seen that the essential piece of non dimensional frequency against the thickness which variety in Electric parameter E and furthermore a similar which shows in hydrostatic pressure. From this, it is seen that the conduct of electric parameter is focused on at hollow cylinder. The idea of non-dimensional frequency against hydrostatic pressure (p_0=-5, 0, 5×10^6) consequently watched.

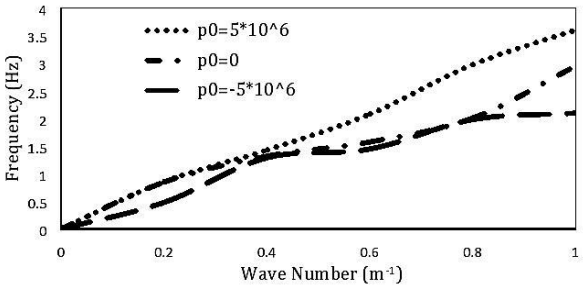

Fig. 6. Variation of frequency vs. wave number against hydrostatic stress p0 with $E = 0$

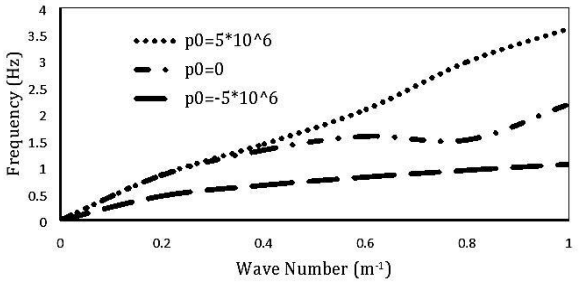

Fig. 7. Variation of frequency vs wave number against hydrostatic stress p0 with $E = 0.5$.

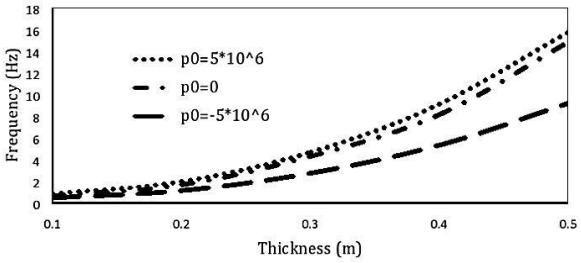

Fig. 8. Variation of frequency versus Thickness against hydrostatic stress p0 with $E = 0$.

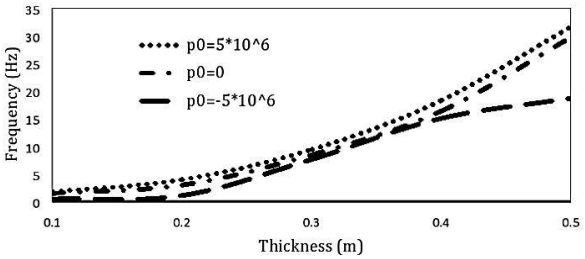

Fig. 9. Variation of frequency versus Thickness against hydrostatic stress p0 with $E = 0.5$.

The non-dimensional frequency versus the thickness h against the with and without hydrostatic stress are plotted in 3D Figs 10-13, which illustrate the effects of the initial hydrostatic stress on the longitudinal vibrations of a LEMV and CFRP layers of the hollow circular cylinder. From the Figs 10 and 11 compared that the LEMV and CFRP layers how to vary without hydrostatic stress for increasing in thickness of the cylinder. From the Figs 12 and 13 compared that the LEMV and CFRP layers how to vary with hydrostatic stress ($p_0 = 5 \times 10^6$) for increasing of thickness of the cylinder. In both cases a linear nature observed in LEMV layers against the influences of with and without hydrostatic stress, but small deviations noted in CFRP layers against the influences of with and without hydrostatic stress.

The 3D Figs: 14-15 shows the non-dimensional strain against the wave number and thickness h, which illustrate the effects of the initial hydrostatic stress on the longitudinal vibrations of a hollow circular cylinder for the value of thermal parameter β.

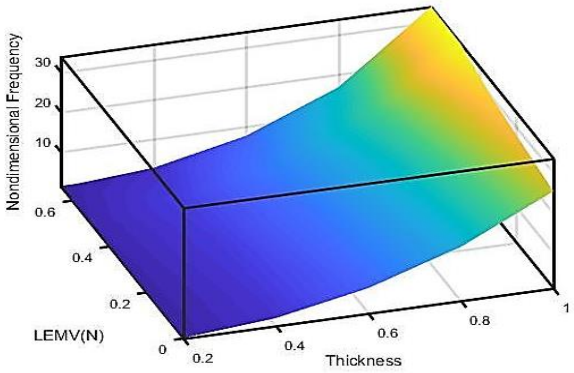

Fig.10. Variation of nondimensional frequency versus thicness of cylinder with LEMV Layer and without hydtrostatic stress.

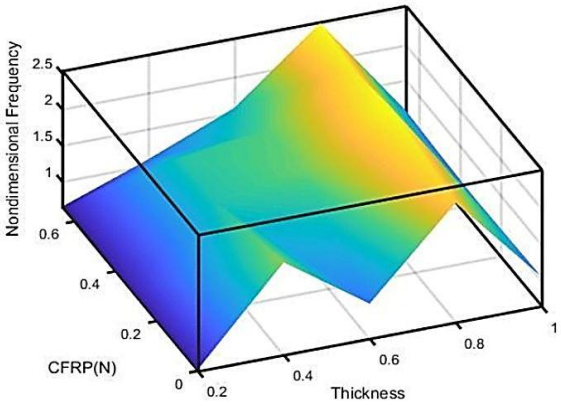

Fig. 11. Variation of nondimensional frequency versus thickness of cylinder with CFRP layer and without hydrostatic stress.

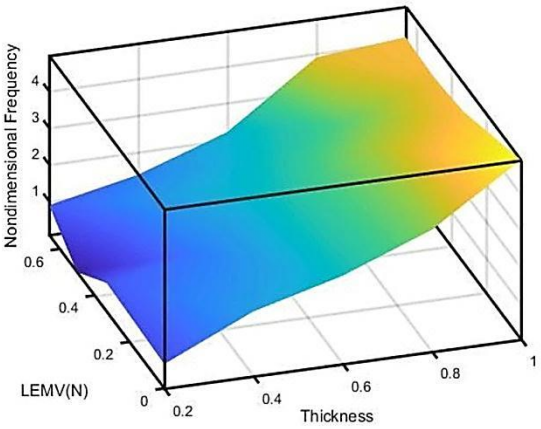

Fig. 12. Variation of nondimensional frequency versus thickness of the cylinder against hydrostatic stress in LEMV layer.

6. Conclusions

The frequency equation for free axisymmetric vibration of the hollow circular cylinder with initial hydrostatic stress as core material is derived using three-dimensional linear theory of elasticity. Three displacement potential func-

tions introduced to uncouple the equations of motion, electric and heat conduction. The frequency equation of the system consisting of rotating piezothermoelastic cylinder developed under the assumption of thermally insulated and electrically shorted free boundary conditions at the surface of the cylinder. The analytical equations numerically studied through the MATLAB programming for axisymmetric modes of vibration for PZT-5A material. The Dispersion curves shows the variation of the various physical parameters of the hollow circular cylinders with a rotation speed, thermal and electrical impacts. The damping observed is not significant due to the rotating effect of the circular hollow cylinder and the presence hydrostatic stress. In addition, the damping observed significant due to the thermal and electric effect of the circular hollow cylinder. The scattering of the frequency in LEMV and CFRP layers are observed in the presence of hydrostatic stress. The methods used in the present article are applicable to a wide range of problems in elasticity with different bonding layers.

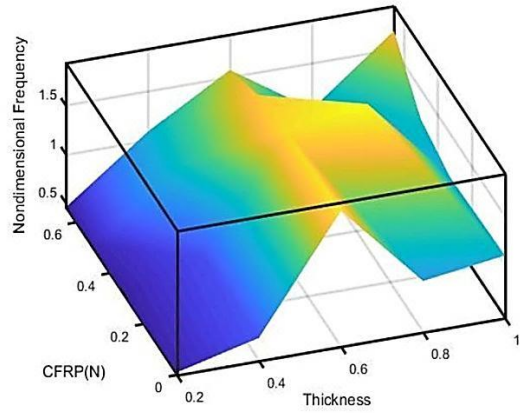

Fig: 13. Variation of nondimensional frequency versus thickness of the cylinder against hydrostatic stress in CFRP layer.

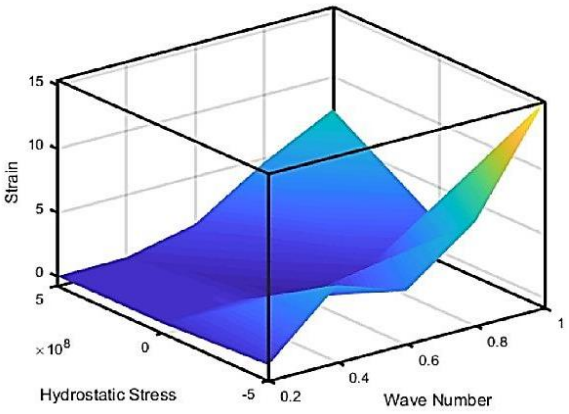

Fig.14. Variation of Strain versus wave number against hydrostatic stress p0 with thermal parameter β.

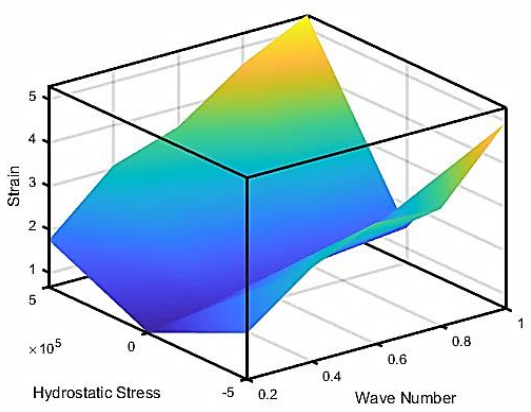

Fig.15. Variation of Strain versus wave number against hydrostatic stress p0 without thermal parameter β.

Reference

[1] Soniya Chaudhary, Sanjeev A. Sahu, Abhinav Singhal, 2018. On secular equation of SH waves propagating in pre-stressed and rotating piezo-composite structure with imperfect interface. *Journal of intelligent material system and structures*, 29, 18.

[2] Soniya Chaudhary, Sanjeev. A Sahu, Abhinav Singhal and Sonal Nirwal, 2019. Interfacial imperfection study in pres-stressed rotating multiferroic cylindrical tube with wave vibration analytical approach. *Materials Research Express*, 10.

[3] Kh. Lotfy, A. El-Bary, 2019. A photothermal excitation for a semiconductor medium due to pulse heat flux and volumetric source of heat with thermal memory. *Waves in Random and Complex Media*.

[4] Kh. Lotfy, 2019. A novel model for photothermal excitation of variable thermal conductivity semiconductor elastic medium subjected to mechanical ramp type with two-temperature theory and magnetic feld. *Scientific Reports*, 9, 3319.

[5] Soniya Chaudhary, Sanjeev A Sahu, Abhinav Singhal and Sonal Nirwal, 2019. Anatomy of flexoelectricity in micro plates with dielectrically highly/weakly and mechanically complaint interface. *Materials Research Express*, 6, 10.

[6] Ebrahimi, F., Karimiasl, M., Singhal, A., 2019. Magneto-electro-elastic analysis of piezoelectric–flexoelectric nanobeams rested on silica aerogel foundation. *Engineering with Computers,* 325.

[7] Abhinav Singhal , Soniya Chaudhary, 2019. Mechanics of 2D elastic stress waves propagation impacted by concentrated point source disturbance in composite material bars, *Journal of Applied and Computational Mechanics*, 6(4).

[8] Kh. Lotfy, 2018. A novel model of photothermal diffusion (PTD) for polymer nano-

composite semiconducting of thin circular plate. *Physica B: Condensed Matter*, 537, pp.320-328.

[9] Placidi, L, and Hutter, K., 2004. Thermodynamics of Polycrystalline materials treated by the theory of mixtures with continuous diversity. *Continuum Mechnaics Thermodynamics*, 17, pp. 409–451.

[10] Altenbach, H, and Eremeyev, 2014. Vibrtion analysis of non-linear 6-parameter prestressed shells. *Meccanica*, 49, pp.1751–1762.

[11] Sonal Nirwal, Sanjeev A.Sahu, Abhinav Singhal Juhi Baroi, 2019. Analysis of different boundary types on wave velocity in bedded piezo-structure with flexoelectric effect. *Composites* Part *B:* Engineering, 167, 434-447.

[12] Kh.Lotfy and Wafaa Hassan, 2013. Effect of rotation for two-temperature generalized thermoelasticity of two-dimensional under thermal shock problem. *Mathematical Problems in Engineering*, pp.13-20.

[13] Abhinav Singhal, Sanjeev A.Sahu, Soniya Chaudhary, 2018. Liouville-Green approximation: An analytical approach to study the elastic wave's vibrations in composite structure of piezo material. *Composite Structures* , 184, pp.714-727.

[14] Soniya Chaudhary, Sanjeev A. Sahu and Abhinav Singhal, 2017. Analytic model for Rayleigh wave propagation in piezoelectric layer overlaid orthotropic substratum. *Acta Mechanica* ,228, pp. 495-529

[15] Sanjeev A.Sahu, Abhinav Singhal, Soniya Chaudhary, 2018. Surface wave propagation in functionally graded piezoelectric material: An analytical solution. *Journal of intelligent material system and structures,* 23, 3.

[16] I. A. Abbas and M. I. A. Othman, 2012. Generalized thermoelastic interaction in a fiber-reinforced anisotropic half-space under hydrostatic initial stress. *Journal of Vibration and Control,* 18, pp. 175–182.

[17] M. Othman and Kh. Lotfy, 2015. The Influence of Gravity on 2-D Problem of Two Temperatures Generalized Thermoelastic Medium with Thermal Relaxation. *Journal of composite and thermo Nanoscience 2015;* 12(9): 2587-2597.

[18] S. Abo-Dahab, Kh. Lotfy, A. Gohaly. Rotation and Magnetic Field Effect on Surface Waves Propagation in an Elastic Layer Lying overa Generalized Thermoelastic Diffusive Half-Space with Imperfect Boundary. *Mathematical Problems in Engineering*.

[19] A. D. Hobinyand I. A. Abbas, 2016, Analytical solution of magneto-thermoelastic interaction in a fiber-reinforced anisotropic material. *European Physical Journal plus, 7,* pp. 131-424.

[20] Manoj Kumar Singh, Sanjeev A Sahu, Abhinav Singhal, Soniya Chaudhary, 2018. Approximation of surface wave velocity in smart composite structure using Wentzel–Kramers–Brillouin method. *Journal of intelligent material system and structures,* 29, 18.

[21] M. A. Othman, S. M. Abo-Dahab, and Kh. Lotfy., 2014. Gravitational effect and initial stress on generalized magneto-thermomicrostretch elastic solid for different theories. *Applied Mathematics and Computation, 230:* pp. *597-615.*

[22] S. M. Abo-Dahab, Kh. Lotfy, 2017. Two-temperature plane strain problem in a semiconducting medium under photo thermal theory. Waves in Random and Complex Media, 27(1), pp. 67-91.

[23] S. M. Abo-Dahab, 2011. Reflection of P and SV waves from stress-free surface elastic half-space under influence of magnetic field and hydrostatic initial stress without energy dissipation. *Journal of vibration control, 17*, pp.*2213–2221.*

[24] Soniya Chaudhary, Sanjeev A. Sahu, Nidhi Dewangan, Abhinav Singhal, 2018. Stresses produced due to moving load in a prestressed piezoelectric substrate. *Mechanics of Advanced Materials and Structures* , 26, pp.1028-1041.

[25] Abhinav Singhal, Sanjeev A.Sahu, Soniya Chaudhary, 2018.Approximation of surface wave frequency in piezo-composite structure. *Composites Part B: Engineering* , 144, pp. 19-28.

[26] Alireza Mohammadi , Hadi Lashini, Mostafa Habibi and Hamed Safarpour, 2019.Influence of viscoelastic foundation on dynamic behaviour of the double walled cylindrical inhomogeneous micro shell using MCST and with the aid of GDQM. *Journal of Solid Mechanics,* 11(2), pp. 440-453.

[27] Ebrahimi F, Hashemabadi D, Habibi M., 2020. Thermal buckling and forced vibration characteristics of a porous GNP reinforced nanocomposite cylindrical shell. *Microsystem Technology,* 26, pp.461–473.

[28] Habibi M, Hashemabadi D and Safarpour H., 2019. Vibration analysis of a high-speed rotating GPLRC nanostructure coupled with a piezoelectric actuator, *The European Physical Journal Plus,* 134, 307.

[29] MostafaHabibi , AlirezaTaghdir , Hamed-Safarpour,2019. Stability analysis of an electrically cylindrical nanoshell reinforced with graphene nanoplatelets. *Composites Part B: Engineering* , 175, pp.107-125.

[30] Mehran Safarpoura, AriaGhabussib, FarzadEbrahimic, et.al. Frequency characteristics of FG-GPLRC viscoelastic thick annular plate with the aid of GDQM. *Thin-Walled Structures,* 150, pp.1066-83.

[31] Abo-el-nour N Abd-alla, Fatimah Alshaikh A., 2015. Mathematical model for longitudinal wave propagation in a magnetoelastic hollow circular cylinder of anisotropic material under the influence of initial hydrostatic stress. *Mathematics and Mechanics of Solids*, pp.1-15.

[32] R. Selvamani and Ponnusamy, 2014. Wave propagation in a transversely isotropic magneto-electro-elastic solid bar immersed in an inviscid fluid. *Journal of the Egyptian Mathematical Society,* 24, pp.92-99.